Journal of Alloys and Compounds 509 (2011) 2981–2985

Contents lists available at ScienceDirect

Journal of Alloys and Compounds

journal homepage: www.elsevier.com/locate/jallcom

Syntheses and characterization of two new selenides $Ba_5Al_2Se_8$ and $Ba_5Ga_2Se_8$

Dajiang Mei[a,b,c], Wenlong Yin[a,b,c], Zheshuai Lin[a,b], Ran He[a,b,c], Jiyong Yao[a,b,*], Peizhen Fu[a,b], Yicheng Wu[a,b]

[a] Center for Crystal Research and Development, Technical Institute of Physics and Chemistry, Chinese Academy of Sciences, Beijing 100190, PR China
[b] Key Laboratory of Functional Crystals and Laser Technology, Chinese Academy of Sciences, Beijing 100190, PR China
[c] Graduate University of Chinese Academy of Sciences, Beijing 100049, PR China

ARTICLE INFO

Article history:
Received 29 September 2010
Received in revised form
23 November 2010
Accepted 25 November 2010
Available online 3 December 2010

Keywords:
Selenide
Synthesis
Crystal structure
Optical
Band structure

ABSTRACT

Two new barium selenides $Ba_5Al_2Se_8$ and $Ba_5Ga_2Se_8$ have been synthesized by solid-state reactions. The structures of $Ba_5Ga_2Se_8$ and $Ba_5Al_2Se_8$ were determined by single-crystal X-ray diffraction method and the Rietveld method, respectively. The two isostructural compounds crystallize in space group *Cmca* of the orthorhombic system with isolated MSe_4 (M = Al, Ga) tetrahedra separated by Ba atoms. The optical band gap of 2.51(2) eV for $Ba_5Ga_2Se_8$ was deduced from the diffuse reflectance spectrum. Band structure calculation indicates that $Ba_5Ga_2Se_8$ is a direct-gap semiconductor. The valence band maximum is dominated by Se 4p orbitals, while the Ba 5d orbitals have the largest contribution to bottom of the conduction band.

1. Introduction

Chalcogenides are an interesting class of materials with amazing structural complexity [1–6] and important properties including thermoelectricity [7–10], magnetic property [11–14], nonlinear optical property [15,16], photovoltaicity [17], superconductivity [18], and luminescent property [19,20]. In the past years, many ternary chalcogenides in the A/M/Q system (A = alkaline-earth metal; M = Al, Ga, In; Q = S, Se, Te) have been discovered and studied, including the large family of the AM_2Q_4 compounds [21–25], the $A_2M_2Q_5$ compounds [26], $Ba_5Ga_2S_8$ [27], $Ba_4Ga_2S_7$ [28], $Ba_3Ga_2S_6$ [28], and $Mg_5Al_2Se_8$ [29]. Extensive investigation has been carried out on the luminescent properties of these compounds doped with rare earth activators since 1970 and some were found to exhibit very attractive luminescent properties [30–33]. For example, Eu^{2+}-activated barium thioaluminate, $BaAl_2S_4$:Eu^{2+}, was one of the most promising materials for the blue component in full-colour inorganic electroluminescent (iEL) display [33–35].

Recently, two new infrared nonlinear optical materials, namely $BaGa_4S_7$ and $BaGa_4Se_7$, have been discovered in the A/M/Q system by Lin et al. [36] and our group [37], respectively. $BaGa_4Se_7$ and $BaGa_4S_7$ crystallize in different structure types (space groups: $Pmn2_1$ vs. Pc) [36–38], although they possess the same composition, which demonstrates the influence of cation/anion size ratio on crystal structures. Here, we report the successful syntheses of two new compounds $Ba_5Al_2Se_8$ and $Ba_5Ga_2Se_8$ as a result of our continuing exploratory investigation in the A/M/Q system. In addition, we report the experimental band gap and electronic structure of $Ba_5Ga_2Se_8$.

2. Experimental

2.1. Solid-state syntheses

The following reagents were used as obtained: Ba (Sinopharm Chemical Reagent Co., Ltd., 98%), Ga (Sinopharm Chemical Reagent Co., Ltd., 99%), Al (Sinopharm Chemical Reagent Co., Ltd., 99%), and Se (Sinopharm Chemical Reagent Co., Ltd., 99%). The binary starting materials, BaSe and M_2Se_3 (M = Al, Ga), were synthesized by stoichiometric reactions of elements in sealed silica tubes evacuated to 10^{-3} Pa at annealing temperatures of 950 °C for BaSe, 800 °C for Al_2Se_3, and 900 °C for Ga_2Se_3, respectively.

Polycrystalline samples of $Ba_5M_2Se_8$ (M = Al, Ga) were synthesized by solid-state reaction techniques. Reaction mixtures of BaSe and M_2Se_3 in the molar ratio of 5:1 were ground and loaded into fused-silica tubes under an Ar atmosphere in a glovebox, which were sealed under 10^{-3} Pa atmosphere and then placed in a computer-controlled furnace. The samples were heated to 950 °C in 20 h, kept at that temperature for 72 h, and then the furnace was turned off.

X-ray powder diffraction analyses of the resultant powder samples were performed at room temperature in the angular range of 2θ = 10–70° with a scan step width of 0.02° and a fixed counting time of 1 s/step using an automated Bruker D8 X-ray diffractometer with graphite monochromatized Cu K_α radiation (λ = 1.5418 Å). The experimental powder X-ray diffraction patterns of $Ba_5Al_2Se_8$ and $Ba_5Ga_2Se_8$ were quite similar to each other, but did not match any pattern in the database and were later found to be in agreement with the calculated pattern on the basis of the single crystal crystallographic data of $Ba_5Ga_2Se_8$ (Fig. 1).

* Corresponding author. Tel.: +86 10 82543725; fax: +86 10 82543725.
E-mail address: jyao@mail.ipc.ac.cn (J. Yao).

0925-8388/$ – see front matter © 2010 Elsevier B.V. All rights reserved.
doi:10.1016/j.jallcom.2010.11.178

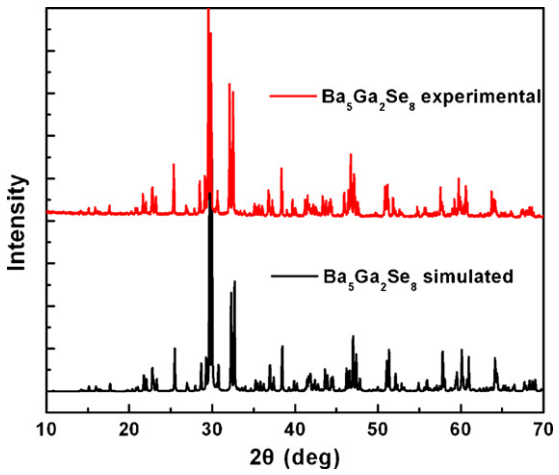

Fig. 1. Experimental (top) and simulated (bottom) powder diffraction patterns of $Ba_5Ga_2Se_8$.

2.2. Single-crystal growth

The as-prepared $Ba_5Ga_2Se_8$ powder was loaded into a fused-silica tube under an Ar atmosphere in a glovebox, which was sealed under 10^{-3} Pa atmosphere and then placed in a computer-controlled furnace. The sample were heated to 1050 °C in 20 h and kept at that temperature for 48 h, then cooled at a slow rate of 1 °C/h to 750 °C, and finally cooled to room temperature. The product consisted of yellow crystals of $Ba_5Ga_2Se_8$, which were manually selected for structure characterization. Analyses of the crystals with an EDX-equipped Hitachi S-3500 SEM showed the presence of Ba, Ga, and Se in the approximate molar ratio of 5:2:8. The crystals are stable in air.

The crystal growth experiment of $Ba_5Al_2Se_8$ was tried in a similar manner at 1100 °C, the highest temperature available in our equipment. However, the powder sample of $Ba_5Al_2Se_8$ did not melt at that temperature and no crystals were obtained. Because the X-ray powder diffraction pattern of $Ba_5Al_2Se_8$ is almost the same as that of $Ba_5Ga_2Se_8$, the structure of $Ba_5Al_2Se_8$ was analyzed by the Rietveld refinement based on the $Ba_5Ga_2Se_8$ structure model.

2.3. Structure determination of $Ba_5Ga_2Se_8$

Single-crystal X-ray diffraction data were collected with the use of graphite-monochromatized Mo K_α (λ = 0.71073 Å) at 93 K on a Rigaku AFC10 diffractometer equipped with a Saturn CCD detector. Crystal decay was monitored by re-collecting 50 initial frames at the end of data collection and no detectable crystal decay was observed. The collection of the intensity data was carried out with the program Crystalclear [39]. Cell refinement and data reduction were carried out with the use of the program Crystalclear [39], and face-indexed absorption correction was performed numerically with the use of the program XPREP [40].

The structure was solved with Direct Methods implemented in the program SHELXS and refined with the least-squares program SHELXL of the SHELXTL.PC suite of programs [40]. The final refinement included anisotropic displacement parameters and a secondary extinction correction. The program STRUCTURE TIDY [41] was then employed to standardize the atomic coordinates. Additional details and structural data are given in Tables 1–3 and further information may be found in Supplementary Material.

Table 1
Crystal data and structure refinements for $Ba_5Ga_2Se_8$ and $Ba_5Al_2Se_8$.

	$Ba_5Ga_2Se_8$	$Ba_5Al_2Se_8$
fw	1457.82	1372.29
a (Å)	23.433(5)	23.4408(4)
b (Å)	12.461(3)	12.5091(2)
c (Å)	12.214(2)	12.2497(3)
Space group	*Cmca*	*Cmca*
V (Å^3)	3567(1)	3591.9(2)
Z	8	8
T (K)	93(2)	298(2)
λ (Å)	0.71073	1.5418
ρ_c (g/cm^3)	5.430	5.079
μ (cm^{-1})	301.32	
R(F), $R_W(F_o^2)$ (SHELX)	0.0342, 0.1018	
R_p, R_{wp} (GSAS)		0.1001, 0.1446

Table 2
Atomic coordinates and equivalent isotropic displacement parameters (Å^2) for $Ba_5Ga_2Se_8$.

Atom	x	y	z	U_{eq} [a]
Ba1	0.09997(2)	0.00324(3)	0.34431(3)	0.00267(9)
Ba2	0.09675(2)	0.15770(3)	0.00495(3)	0.00246(9)
Ba3	1/4	0.25453(4)	1/4	0.0064(1)
Ga1	0	0.31321(7)	0.23017(8)	0.0024(2)
Ga2	0.25016(4)	0	0	0.0024(2)
Se1	0	0.47699(7)	0.34826(7)	0.0026(2)
Se2	0.18647(3)	0.00066(4)	0.15195(5)	0.0042(1)
Se3	0.18708(3)	0.34850(5)	0.00175(5)	0.0037(1)
Se4	0.09304(3)	0.24493(4)	0.25749(5)	0.0029(1)
Se5	0	0.35385(7)	0.03129(7)	0.0027(2)

[a] U_{eq} is defined as one third of the trace of the orthogonalized U_{ij} tensor.

Table 3
Interatomic distances (Å) for $Ba_5Ga_2Se_8$.

Atoms	Distances	Atoms	Distances	Atoms	Distances
Ga1–Se4	2.3640(8)	Ba1–Se3	3.3583(8)	Ba2–Se1	3.6641(9)
Ga1–Se4	2.3640(8)	Ba1–Se3	3.3794(8)	Ba3–Se3	3.5692(8)
Ga1–Se5	2.482(1)	Ba1–Se4	3.4544(9)	Ba3–Se3	3.5692(8)
Ga1–Se1	2.499(1)	Ba1–Se5	3.7248(9)	Ba3–Se2	3.6134(9)
Ga2–Se2	2.3816(9)	Ba2–Se3	3.1834(9)	Ba3–Se2	3.6134(9)
Ga2–Se2	2.3816(9)	Ba2–Se4	3.2582(9)	Ba3–Se3	3.6439(8)
Ga2–Se3	2.3933(9)	Ba2–Se4	3.2716(9)	Ba3–Se3	3.6439(8)
Ga2–Se3	2.3933(9)	Ba2–Se5	3.3494(9)	Ba3–Se4	3.681(1)
Ba1–Se2	3.1033(9)	Ba2–Se2	3.3871(8)	Ba3–Se4	3.681(1)
Ba1–Se4	3.1971(9)	Ba2–Se1	3.4088(8)	Ba3–Se2	3.6957(9)
Ba1–Se1	3.3356(9)	Ba2–Se2	3.4620(8)	Ba3–Se2	3.6957(9)
Ba1–Se5	3.3557(8)				

2.4. Structure determination of $Ba_5Al_2Se_8$

The X-ray powder diffraction pattern of $Ba_5Al_2Se_8$ is almost identical with that of $Ba_5Ga_2Se_8$, so the structure of $Ba_5Al_2Se_8$ was analyzed by the Rietveld refinement on the basis of the $Ba_5Ga_2Se_8$ structure model with the use of the EXPGUI and GSAS program packages [42,43]. A Le Bail refinement was first performed to refine the terms for background function, unit cell parameters, zero point error, and profile coefficients, and then the Rietveld refinement was carried out to include the refinements of the scale factor, atomic positions, and thermal parameters. The last set of refinement yielded to a value of R_p = 0.1001 and R_{wp} = 0.1446. The refined cell parameters of $Ba_5Al_2Se_8$ are a = 23.4408(4) Å, b = 12.5091(2) Å, c = 12.2497(3) Å, and V = 3591.9(2) Å^3 at 298 K, whereas those of $Ba_5Ga_2Se_8$ are a = 23.4700(9) Å, b = 12.5244(4) Å, c = 12.2650(4) Å, and V = 3605.3(3) Å^3 at 298 K based on the X-ray powder diffraction pattern of $Ba_5Ga_2Se_8$. The final refinement pattern of $Ba_5Al_2Se_8$ is given in Fig. 2 and selected crystallographic data are reported in Table 1.

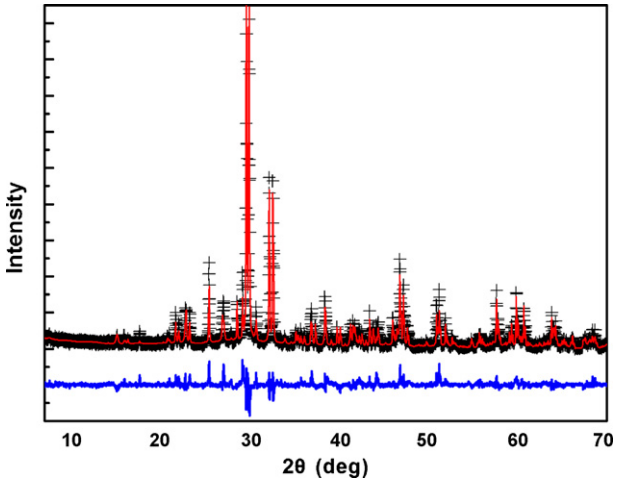

Fig. 2. Calculated (−), experimental (+) and difference (lower horizontal line) profiles from Rietveld refinement of ambient temperature XRD data for $Ba_5Al_2Se_8$.

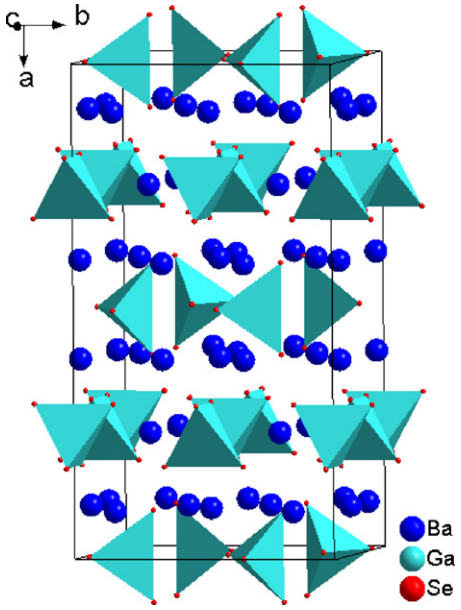

Fig. 3. Unit cell of the $Ba_5Ga_2Se_8$ structure.

2.5. Diffuse reflectance spectroscopy

A Cary 1E UV-visible spectrophotometer with a diffuse reflectance accessory was used to measure the spectrum of $Ba_5Ga_2Se_8$ in the range of 350 nm (3.54 eV)–850 nm (1.46 eV).

2.6. Band structure calculation

The electronic structure calculation was performed using the first principles plane-wave pseudopotential method [44] implemented in the CASTEP package [45]. Normal-conserving pseudopotentials [46,47] were used with the Se 4s, Se 4p, Ba 5s, Ba 5p, Ba 5d, Ba 6s, Ga 3d, Ga 4s, and Ga 4p electrons treated as valence electrons. Local-density approximation (LDA) with a kinetic energy cutoff of 600 eV was adopted and Monkhorst–Pack [48] *k* point meshes with a density of $(2 \times 2 \times 2)$ points in the Brillouin zone of the unit cell were used.

3. Results and discussion

3.1. Syntheses

$Ba_5Ga_2Se_8$ single crystals were grown by the spontaneous nucleation method and powder sample of $Ba_5Al_2Se_8$ was successfully synthesized at 950 °C. Efforts to synthesize analogues, in the form of either single crystals or polycrystalline samples, with other alkaline-earth metal, group III metal, or chalcogen were not successful. The products of similar reactions were mixtures of the ternary AM_2Q_4 and the binary AQ compounds, which indicate that the relative cation/anion size ratio has obvious influence on the stability of the crystal structures.

3.2. Structure

$Ba_5Ga_2Se_8$ crystallizes in space group *Cmca* of the orthorhombic system and adopts the $Ba_5Ga_2S_8$ structure type [27]. As shown in Fig. 3, the structure consists of isolated $GaSe_4$ tetrahedra separated by Ba atoms. The asymmetric unit contains three crystallographically independent Ba atoms, two independent Ga atoms, and five independent Se atoms. Ba1 and Ba2 atoms are coordinated to a bicapped trigonal prism of eight Se atoms with the Ba–Se distances ranging from 3.1033(9) to 3.7248(9) Å, while Ba3 is coordinated to a larger polyhedron of ten Se atoms with the Ba–Se distances ranging from 3.5692(8) to 3.6957(9) Å. These Ba–Se distances are close to those in $BaGa_4Se_7$ (3.429(2) to 3.861(2) Å) [37] and $BaNb_{0.8}Se_3$ (3.559(2) to 3.584(2) Å) [49]. Each Ga atom is coordinated to a slightly distorted tetrahedron of four Se atoms. The Ga–Se distances range from 2.3640(8) to 2.499(1) Å, which are comparable to those of 2.361(2)–2.488(2) Å in $BaGa_4Se_7$ [37]. Since there are no Se–Se bonds in the structures, the oxidation states of 2+, 3+, and 2− can be assigned to Ba, Ga, and Se, respectively.

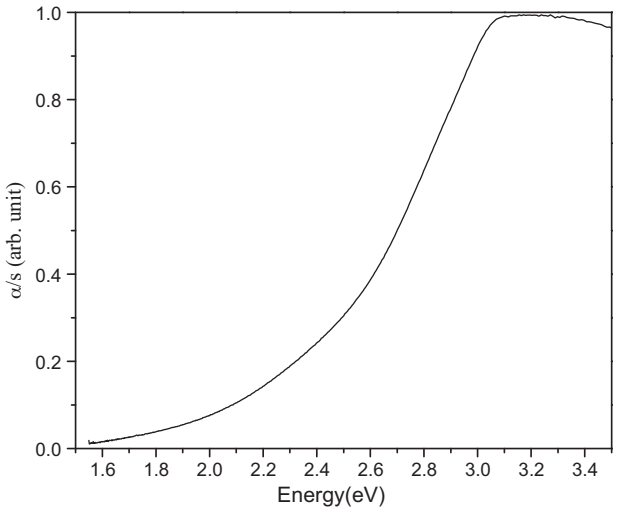

Fig. 4. Diffuse reflectance spectrum of $Ba_5Ga_2Se_8$.

Two other compounds, namely $Ba_5Ga_2S_8$ and $Mg_5Al_2Se_8$, were reported to possess the $A_5M_2Q_8$ composition in the A/M/Q (A = alkaline-earth metal, M = Al, Ga, In; Q = S, Se, Te) system [27,29]. $Ba_5Ga_2S_8$, $Ba_5Ga_2Se_8$, and $Ba_5Al_2Se_8$ are isostructural, while $Mg_5Al_2Se_8$ crystallizes in a different space group $Pna2_1$. As a result of its much smaller radius, Mg is coordinated to an octahedron of six Se atoms at distances between 2.397 and 3.077 Å in $Mg_5Al_2Se_8$ [29]. However, the arrangement of $AlSe_4$ tetrahedra in $Mg_5Al_2Se_8$ is similar to that of $GaSe_4$ in $Ba_5Ga_2Se_8$, i.e. they are also completely separated from each other. The complete isolation of the MQ_4 tetrahedra is uncommon in the A/M/Q system as in all other compounds; the MQ_4 tetrahedra are connected to each other in one way or another. For example, all $GaSe_4$ tetrahedra are linked to each other to generate a three-dimensional framework with cavities occupied by Ba atoms in $BaGa_4Se_7$ [37]; the $InSe_4$ tetrahedra are connected through corner and edge-sharing to form two-dimensional layers in $BaIn_2Se_4$ [50]; and the edge-shared $GaSe_4$ tetrahedra form one-dimensional chains in $BaGa_2Se_4$ [21]. It is reasonable that the lower the content of M in the structure is, the sparser the MSe_4 tetrahedra connectivity will be. The M/A ratio in the $A_5M_2Se_8$ compounds is smallest among all compounds found in the A/M/Q system and so their MSe_4 tetrahedra are completely separated by A atoms in the structures.

3.3. Experimental band gap

The diffuse reflectance spectrum of $Ba_5Ga_2Se_8$ is shown in Fig. 4. A band gap of 2.51(2) eV was deduced by the straightforward extrapolation method [51].

3.4. Band structure calculation

The calculated band structure of the $Ba_5Ga_2Se_8$ is plotted along the high symmetry lines in Fig. 5. The energy band can be divided into three regions: the lower region located below −4 eV (not displayed), the valence band (VB) from about −4 to 0 eV, and the conduction band (CB) in which a band of a dispersion spanning about 0.4 eV appears at the bottom of its conduction bands from

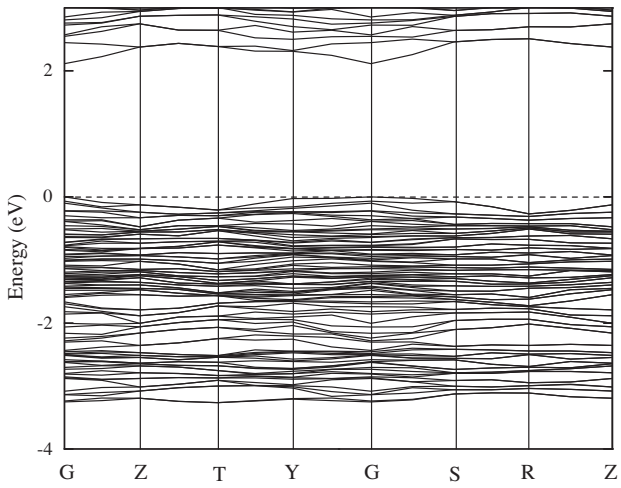

Fig. 5. Band structure of $Ba_5Ga_2Se_8$ along the lines of high symmetry points in the Brillouin zone. The dash line indicates the VB maximum.

the G point to the S point. The calculated direct band gap is 2.18 eV, which is in reasonable agreement with experimental result from the diffuse reflectance spectrum. The results did not change if other kinds of pseudopotentials were used for the calculations.

The partial density of states (PDOS) projected on the constitutional atoms shows that the Ba 6s and Ga 3d orbitals are strongly localized in the very deep region of the VB at about −28 eV and −15 eV, respectively, and the VB from −13 eV to −10 eV are mainly composed of the Ba 5p orbitals (not shown). Thus these orbitals have no chemical bonding with other atoms. Fig. 6 gives the PDOS above −8 eV, in which several electronic characteristics can be seen: (i) the upper part of the valence band from −6 eV to −2 eV show a large hybridization between Ga 4p (and 4s) and Se 4p orbitals, indicating the quite strong chemical bonds between the Ga and Se atoms. (ii) At the top of valence states (above −3.5 eV) some Ba 5d orbitals occur, and also have some hybridization with the Se 4p orbitals, which means that there exists some chemical bonding between barium and selenium in $Ba_5Ga_2Se_8$. (iii) The valence band maximum is dominated by Se 4p orbitals, while the bottom of CB is composed of the orbitals of Ba, Se, and Ga atoms with the Ba 5d orbitals exhibiting the largest contribution.

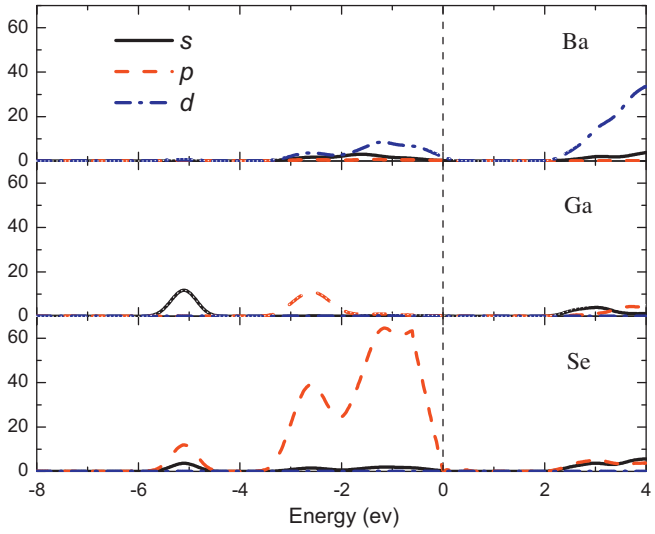

Fig. 6. Partial density of states of $Ba_5Ga_2Se_8$. The solid, dot-dash, and dash lines are the s, p, and d orbitals, respectively. The broken vertical lines indicate the VB maximum.

It is interesting to mention that Ba 5d orbitals have significant contribution to the energy bands around Fermi level in $Ba_5Ga_2Se_8$ since they have some hybridization with the Se 4p orbitals at the top of VB and dominate the bottom of the CB. In comparison, the Ba 5d orbitals only have a little contribution to the higher electronic levels of CB and are negligible at the top of the VB in $BaGa_4Se_7$ [37].

4. Conclusions

Two new barium selenides $Ba_5Al_2Se_8$ and $Ba_5Ga_2Se_8$ have been synthesized for the first time. They crystallize in space group *Cmca* of the orthorhombic system and are isostructural with $Ba_5Ga_2S_8$. The structures feature isolated MSe_4 (M = Al, Ga) tetrahedra separated by Ba atoms. The optical band gap was determined to be 2.51 (2) eV for $Ba_5Ga_2Se_8$ with the use of the diffuse reflectance spectrum measurement. The electronic structure calculation indicates that $Ba_5Ga_2Se_8$ is a direct-gap semiconductor. The valence band maximum is dominated by Se 4p orbitals, whereas the Ba 5d orbitals have the largest contribution to bottom of the conduction band.

Acknowledgments

This research was supported by the National Basic Research Project of China (No. 2010CB630701). ZSL acknowledges the Special Foundation of President of Chinese Academy of Sciences.

Appendix A. Supplementary data

Supplementary data associated with this article can be found, in the online version, at doi:10.1016/j.jallcom.2010.11.178.

References

[1] F.Q. Huang, P. Brazis, C.R. Kannewurf, J.A. Ibers, J. Am. Chem. Soc. 122 (2000) 80.
[2] Y. Wu, W. Bensch, Inorg. Chem. 48 (2009) 2729.
[3] F.Q. Huang, J. Yao, J. Yang, J.A. Ibers, J. Alloys Compd. 462 (2008) 38.
[4] V.R. Kozer, A.O. Fedorchuk, I.D. Olekseyuk, O.V. Parasyuk, J. Alloys Compd. 503 (2010) 40.
[5] A. Gour, S. Singh, J. Alloys Compd. 504 (2010) 427.
[6] D. Mei, Z. Lin, L. Bai, J. Yao, P. Fu, Y. Wu, J. Solid State Chem. 183 (2010) 1640.
[7] L.R. Testardi Jr., J.N. Bierly, F.J. Donahoe, J. Phys. Chem. Solids 23 (1962) 1209.
[8] D.-Y. Chung, T. Hogan, P. Brazis, M. Rocci-Lane, C. Kannewurf, M. Bastea, C. Uher, M.G. Kanatzidis, Science 287 (2000) 1024.
[9] T. Kyratsi, I. Kika, E. Hatzikraniotis, K.M. Paraskevopoulos, K. Chrissafis, M.G. Kanatzidis, J. Alloys Compd. 474 (2009) 351.
[10] A. Charoenphakdee, K. Kurosaki, A. Harnwunggmoung, H. Muta, S. Yamanaka, J. Alloys Compd. 496 (2010) 53.
[11] J.-H. Chung, K. Ohgushi, Y. Ueda, J. Magn. Magn. Mater. 322 (2010) 832.
[12] R.G. Veliyev, M.Y. Seyidov, N.Z. Gasanov, F.M. Seyidov, J. Alloys Compd. 506 (2010) 800.
[13] O.M. Strok, M. Daszkiewicz, L.D. Gulay, D. Kaczorowski, J. Alloys Compd. 493 (2010) 47.
[14] M. Daszkiewicz, O.M. Strok, L.D. Gulay, D. Kaczorowski, J. Alloys Compd. 508 (2010) 258.
[15] J.D. Feichtner, G.W. Roland, Appl. Opt. 11 (1972) 993.
[16] T.K. Bera, J.I. Jang, J.B. Ketterson, M.G. Kanatzidis, J. Am. Chem. Soc. 131 (2009) 75.
[17] R. Klenk, J. Klaer, R. Scheer, M.C. Lux-Steiner, I. Luck, N. Meyer, U. Ruehle, Thin Solid Films (2005) 480.
[18] S. Margadonna, Y. Takabayashi, M.T. McDonald, K. Kasperkiewicz, Y. Mizuguchi, Y. Takano, A.N. Fitch, E. Suard, K. Prassides, Chem. Commun. 43 (2008) 5607.
[19] L. Solymar, D. Walsh, Electrical Properties of Materials, 6th ed., Oxford University Press, New York, 1998.
[20] P.F. Smet, I. Moreels, Z. Hens, D. Poelman, Materials 3 (2010) 2834.
[21] W. Klee, H. Schaefer, Z. Anorg. Allg. Chem. 479 (1981) 125.
[22] E.R. Franke, H. Schaefer, Z. Naturforsch. B27 (1972) 1308.
[23] B. Eisenmann, M. Jakowski, H. Schaefer, Mater. Res. Bull. 17 (1982) 1169.
[24] B. Eisenmann, M. Jakowski, W. Klee, H. Schaefer, Rev. Chim. Miner. 20 (1983) 255.
[25] B. Eisenmann, M. Jakowski, H. Schaefer, Rev. Chim. Miner. 19 (1982) 263.
[26] B. Eisenmann, A. Hofmann, Z. Anorg. Allg. Chem. 580 (1990) 151.
[27] B. Eisenmann, M. Jakowski, H. Schaefer, Z. Naturforsch. B39 (1984) 27.
[28] B. Eisenmann, M. Jakowski, H. Schaefer, Rev. Chim. Miner. 21 (1984) 12.

[29] K.P. Dotzel, H. Schaefer, Z. Naturforsch. B32 (1977) 1488.
[30] R.B. Jabbarova, C. Chartierb, B.G. Tagieva, O.B. Tagieva, N.N. Musayevaa, C. Barthoub, P. Benalloulb, J. Phys. Chem. Solids 66 (2005) 1049.
[31] M. Marceddu, A. Aneddaa, R. Corpino, A.N. Georgobiani, P.C. Ricci, Mater. Sci. Eng. B 146 (2008) 216.
[32] M. Nazarov, D.-Y. Noh, C.C. Byeon, H. Kim, J. Appl. Phys. 105 (2009) 073518–73521.
[33] Y.H. Cho, R.B.V. Chalapathy, D.H. Park, B.T. Byung, J. Electrochem. Soc. 157 (2010) J45.
[34] N. Miura, M. Kawanishi, H. Matsumoto, R. Nakano, Jpn. J. Appl. Phys. 38 (1999) L1291.
[35] X. Wu, Proceedings of the Twenty-second International Display Research Conference, 2002, p. 353.
[36] X. Lin, G. Zhang, N. Ye, Cryst. Growth Des. 9 (2009) 1186.
[37] J. Yao, D. Mei, L. Bai, Z. Lin, W. Yin, P. Fu, Y. Wu, Inorg. Chem. 49 (2010) 9212.
[38] B. Eisenmann, M. Jakowski, H. Schaefer, Rev. Chim. Miner. 20 (1983) 329.
[39] CrystalClear, Rigaku Corporation, Tokyo, Japan, 2008.
[40] G.M. Sheldrick, Acta Crystallogr. Sect. A 64 (2008) 112.
[41] L.M. Gelato, E. Parthé, J. Appl. Crystallogr. 20 (1987) 139.
[42] A.C. Larson, R.B. Von Dreele, General Structure Analysis System (GSAS), Los Alamos National Laboratory Report LAUR 86-748 (1994).
[43] B.H. Toby, J. Appl. Crystallogr. 3 (2001) 210.
[44] M.C. Payne, M.P. Teter, D.C. Allan, T.A. Arias, J.D. Joannopoulos, Rev. Mod. Phys. 64 (1992) 1045.
[45] S.J. Clark, M.D. Segall, C.J. Pickard, P.J. Hasnip, M.J. Probert, K. Refson, M.C. Payne, Z. Kristallogr. 220 (2005) 567.
[46] A.M. Rappe, K.M. Rabe, E. Kaxiras, J.D. Joannopoulos, Phys. Rev. B 41 (1990) 1227.
[47] J.S. Lin, A. Qseish, M.C. Payne, V. Heine, Phys. Rev. B 47 (1993) 4174.
[48] J.P. Perdew, K. Burke, M. Ernzerhof, Phys. Rev. Lett. 77 (1996) 3865.
[49] T. Ohtani, S. Honji, M. Takano, J. Solid State Chem. 132 (1997) 188.
[50] W. Klee, H. Schaefer, Rev. Chim. Miner. 16 (1979) 465.
[51] O. Schevciw, W.B. White, Mater. Res. Bull. 18 (1983) 1059.